Transform Domain: Design of Closed-Form Joint 2-D DOA Estimation Based on QR Decomposition

Hui Cao, Qi Liu & Yuntao Wu

Circuits, Systems, and Signal Processing

ISSN 0278-081X
Volume 39
Number 10

Circuits Syst Signal Process (2020)
39:5318-5329
DOI 10.1007/s00034-020-01416-8

Springer

Circuits, Systems, and Signal Processing (2020) 39:5318–5329
https://doi.org/10.1007/s00034-020-01416-8

SHORT PAPER

Transform Domain: Design of Closed-Form Joint 2-D DOA Estimation Based on QR Decomposition

Hui Cao[1] · **Qi Liu**[2] · **Yuntao Wu**[3]

Received: 10 January 2020 / Revised: 1 April 2020 / Accepted: 2 April 2020 /
Published online: 21 April 2020

Abstract

As an alternative to existing methods, we design a transform-domain algorithm to avoid the computational cost of a two-dimensional (2-D) spectral peak search when addressing the problem of joint azimuth and elevation directions-of-arrival (DOAs) estimation via an L-shaped array. Motivated by the linear prediction property of the signal cross-covariance matrix, the 2-D DOA estimation problem is equivalently converted into a 2-D frequency estimation problem. With the QR decomposition technique, the closed-form solutions in the transform domain with respect to the azimuth and elevation angles are successively estimated using the weighted least squared method as the solver, and it is shown that the proposed scheme achieves automatically pairing while permitting fast implementation. Simulations are presented to verify the effectiveness of the proposed method by comparison with several 2-D DOA estimators as well as the Cramér–Rao lower bound.

Keywords Direction-of-arrival estimation · Array signal processing · QR decomposition · Closed-form solution

✉ Qi Liu
elelqi@nus.edu.sg

Hui Cao
iehuicao@whut.edu.cn

Yuntao Wu
ytwu@sina.com

1 School of Information Engineering, Wuhan University of Technology, Luoshi Road, Wuhan 430070, China

2 Department of Electrical and Computer Engineering, National University of Singapore, Singapore, Singapore

3 School of Computer Science and Engineering, Wuhan Institute of Technology, Wuhan 430205, China

1 Introduction

Direction-of-arrival (DOA) estimation for multiple narrowband sources has been important for decades due to its broad applications in radar, sonar, radio astronomy, and mobile communications [3,4,10,13,19], and so forth. Many DOA estimators with super-resolution performance have been proposed, but most of them address one-dimensional (1-D) DOA estimation problems, such as [13]. In practice, when an airborne or spaceborne array is employed to observe ground-based sources, the angle of each source is two-dimensional (2-D) in nature, and the corresponding angular components are known as the azimuth and elevation angles. Therefore, 1-D DOA estimators may fail to deal with the joint azimuth and elevation angles estimation problem.

To tackle this 2-D DOA estimation problem, various methods have been developed, such as MUSIC-based method [20] and ESPRIT-based algorithms [8]. These subspace-based algorithms achieve satisfactory estimation performance for various array geometries, including a uniform linear array (ULA), a rectangular array and an L-shaped array. Nevertheless, most of them require a multidimensional search, resulting in a high computational cost. For this reason, a fast computational method that does not require solving for the roots of a 2-D polynomial or searching in 2-D space, called the matrix enhancement and matrix pencil (MEMP) method [6], has been proposed to deal with the 2-D frequency estimation problem. In this method, an enhanced matrix is constructed from data samples, and 2-D sinusoids are then extracted from the principal eigenvectors of the enhanced matrix via the matrix pencil approach.

In [17], a propagator method (PM) has also been developed to reduce the computational complexity; this method requires only linear operations on signal subarrays instead of singular value decomposition (SVD) as in subspace-based methods. In [18], a 2-D DOA estimator based on an L-shaped array was designed by using a parameter finding process similar to MUSIC. However, both of these methods require an extra paired-matching process, which is also true of [14,16]. The work presented in [17] achieves effective pair matching using a signal subspace extension, in which each L-shaped array is composed of two different ULAs. To achieve pair matching, a novel sparse representation-based method [21] for wideband 2-D DOA estimation in the frequency domain has been presented by characterizing individual wideband sources as unique planes of temporal–spatial array data to enable the projection of 2-D direction information into 1-D space. However, the capabilities of this approach are limited for wideband source estimation. The maximum likelihood (ML) method [9] for 2-D localization exhibits optimal performance with relatively lower complexity, and simulation results show that the ML method attains the Cramér–Rao lower bound (CRLB) with super-resolution performance unlike other existing approaches. Other methods for 1-D DOA estimation [11,12,23] and 2-D DOA estimation [2,22,24] have also been proposed to solve the DOA estimation problem.

In this paper, a closed-form 2-D DOA estimator with low computational complexity is proposed, along with the resultant 2-D frequency estimation problem. To deal with the unpair matching problem for joint azimuth and elevation angles, the QR decomposition technique is applied to the autocorrelation covariance matrix of the received data such that 2-D direction information can be decomposed into 1-D frequency estimates

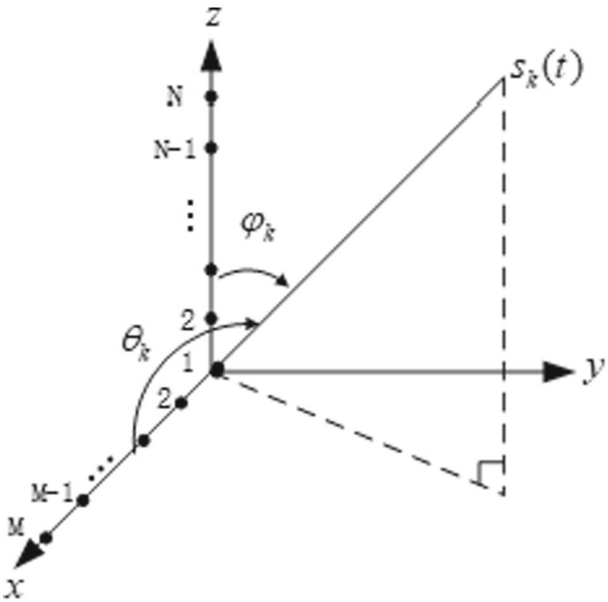

Fig. 1 L-shaped array configuration for 2-D DOA estimation

with respect to (w.r.t.) the elevation angle. Benefiting from the linear prediction (LP) property of signal cross-covariance matrix [5], we address the resulting 1-D frequency estimation problem using the weighted least squared (WLS) method, thus obtaining a closed-form solution w.r.t. the elevation angle. Subsequently, with the help of a constructed steering matrix for the estimated elevation angle, the remaining 1-D frequency problem w.r.t. the azimuth angle is solved in the same manner.

The main contributions of this work are summarized as follows. First, motivated by the LP property of the signal cross-covariance matrix, the 2-D DOA estimation problem is successfully converted into the corresponding 2-D frequency estimation problem, for which closed-form estimates are obtained instead of performing iterative approximation. Second, a multidimensional spectral search is not required, which, in some sense, implies that the proposed scheme is computationally efficient. Furthermore, the proposed solution offers more accurate DOA estimation performance and achieves automatic pair matching between the azimuth and elevation angles.

2 Signal Model

Consider an L-shaped array equipped with identical M sensors along the x-axis and N identical sensors along the z-axis, as shown in Fig. 1. The interelement spacing d is equal to half the wavelength. Without loss of generality, assume that K narrowband sources with signal carrier wavelength λ from the far-field impinge onto the L-shaped array from unknown and distinct angle pairs (θ_k, ϕ_k), $1 \leq k \leq K$. The received signals on the $x - z$ plane along the ULAs are given by

$$\mathbf{x}(t) = \mathbf{A}_x \mathbf{s}(t) + \mathbf{n}_x(t), \quad \mathbf{z}(t) = \mathbf{A}_z \mathbf{s}(t) + \mathbf{n}_z(t), \tag{1}$$

where $\mathbf{s}(t) = [s_1(t), \ldots, s_K(t)]^{\mathrm{T}}$ is the signal vector with the superscript $^{\mathrm{T}}$ being the transpose operator, both $\mathbf{n}_x(t)$ and $\mathbf{n}_z(t)$ are assumed to be additive white Gaussian noises, and the array manifold matrices of the x-ULA and z-ULA are written as:

$$\mathbf{A}_x = [\mathbf{a}_x(\theta_1), \mathbf{a}_x(\theta_2), \ldots, \mathbf{a}_x(\theta_K)], \tag{2}$$

$$\mathbf{A}_z = [\mathbf{a}_z(\phi_1), \mathbf{a}_z(\phi_2), \ldots, \mathbf{a}_z(\phi_K)], \tag{3}$$

where the steering vectors are expressed as $\mathbf{a}_x(\theta_k) = [1, a_k, \ldots, a_k^{M-1}]^{\mathrm{T}}$ and $\mathbf{a}_z(\phi_k) = [1, b_k, \ldots, b_k^{N-1}]^{\mathrm{T}}$ with a_k and b_k being $a_k = \exp(j\mu_k)$ and $b_k = \exp(j\nu_k)$, respectively. Note that $j = \sqrt{-1}$. The variables (μ_k, ν_k), expressed as $\mu_k = 2\pi d \cos\theta_k/\lambda$ and $\nu_k = 2\pi d \cos\phi_k/\lambda$, respectively, are frequency variables corresponding to (θ_k, ϕ_k).

The cross-covariance matrix of $\mathbf{x}$ and $\mathbf{z}$ is defined as:

$$\bar{\mathbf{R}} = \mathbb{E}[\mathbf{x}(t)\mathbf{z}^H(t)] = \mathbf{A}_x \mathbf{S} \mathbf{A}_z^H + \sigma^2 \mathbf{I}_{M\times N}, \tag{4}$$

where the nonsingular diagonal matrix $\mathbf{S} \in \mathbb{C}^{K\times K}$ is computed as $\mathbf{S} = \mathbb{E}[\mathbf{s}(t)\mathbf{s}^H(t)]$ with ^{H} denoting the complex conjugate transpose operator, and σ^2 is the noise power. $\mathbf{I}_{M\times N}$ is an $M \times N$ size of matrix with $\mathbf{I}(i,j) = 1$ when $i = j$, and $\mathbf{I}(i,j) = 0$ otherwise.

3 Algorithm Development

For the ease of readability, we first analyze our developed algorithm in the noise-free case. We define $\mathbf{Y} = \mathbf{A}_x \mathbf{S} \mathbf{A}_z^H$, where the elements of the noise free $\mathbf{Y}$ can be expressed as:

$$\begin{aligned} \mathbf{Y}_{m,n} &= \sum_{k=1}^{K} s_k(t) s_k^H(t) a_k^{m-1} (b_k^*)^{n-1} \\ &= \sum_{k=1}^{K} s_k(t) s_k^H(t) e^{j2\pi d/\lambda[(m-1)\cos\theta_k - (n-1)\cos\phi_k]}, \end{aligned} \tag{5}$$

where * is the conjugate operator. As shown in (5), the cross-covariance matrix $\mathbf{Y}$ depends on not only the azimuth angle-dependent but also the elevation angle. Our idea is first to estimate one of the two angles, ϕ_k (or θ_k), from the cross-covariance matrix of the received signal and then to obtain the other angle, θ_k (or ϕ_k), based on the steering vector information of the estimated ϕ_k (or θ_k). To decrease the effect of the information of the other angle, the autocorrelation covariance matrix is computed as:

$$\mathbf{R}_{yy} = \mathbf{Y}^H \mathbf{Y} = \mathbf{A}_z \mathbf{S}_y \mathbf{A}_z^H, \tag{6}$$

where $\mathbf{S}_y = \mathbf{S}^H \mathbf{A}_x^H \mathbf{A}_x \mathbf{S}$ and its elements are defined as $s_y(m, n), m = 1, \ldots, N - 1, n = 1, \ldots, N-1$. It is worth noting that when computing the autocorrelation covariance matrix, the pairing information of the azimuth and elevation angles contained in $\bar{\mathbf{R}}$ still exists, and the details are shown in [7].

Next, we perform QR decomposition of $\mathbf{R}_{yy}$ [5]:

$$\mathbf{R}_{yy} = \mathbf{QR}, \tag{7}$$

where $\mathbf{Q} \in \mathbb{C}^{M\times M}$ is an orthonormal matrix and $\mathbf{R} \in \mathbb{C}^{M\times N}$ is an upper triangular matrix with $\mathbb{C}$ being the set of complex numbers. Adopting the notation $\mathbf{Q} = \left[\mathbf{q}_1\ \mathbf{q}_2 \cdots \mathbf{q}_M\right]$ and $\mathbf{R} = \left[\mathbf{r}_1\ \mathbf{r}_2 \cdots \mathbf{r}_M\right]^{\mathrm{T}}$, we conclude that $\mathbf{q}_i^{\mathrm{H}}\mathbf{q}_j = 0$ for $i \neq j$, and $\mathbf{q}_i^{\mathrm{H}}\mathbf{q}_j = 1$ otherwise. Since $\mathrm{rank}(\mathbf{R}_{yy}) = K$ and $\mathbf{R}$ is an upper triangular matrix, both $\mathbf{r}_i, i \in \{K+1, \ldots, M\}$ are $\mathbf{0}$, where $\mathbf{0} \in \mathbb{C}^{N\times 1}$ denotes a vector with all 0 values.

The elements along the columns or rows of $\mathbf{R}_{yy}$ satisfy the LP property, that is:

$$\begin{aligned} &u_{m,n} + \sum_{k=1}^{K} c_k u_{m,n-k} = 0, \\ &m = 1, 2, \ldots, N, \quad n = K+1, K+2, \ldots, N, \end{aligned} \tag{8}$$

where $u_{m,n} = \exp(j\nu_m) s_y(m, n) \exp(j\nu_n^*)$ and the $c_k = b_k^*$ are the LP coefficients, from which the ν_k are given by the K roots of the following polynomial [1]:

$$1 + \sum_{k=1}^{K} c_k z^{K-k} = 0, \tag{9}$$

where $z = b_k, k = 1, \ldots, K$. Let $\mathbf{R}_{yy} = \left[\mathbf{u}_1\ \mathbf{u}_2 \cdots \mathbf{u}_N\right]$, with its elements being defined as $\mathbf{u}_k = \left[u_{1,k}\ u_{2,k} \cdots u_{N,k}\right]^T$, then, we have $\mathbf{r}_k = \left[\mathbf{q}_k^H\mathbf{u}_1\ \mathbf{q}_k^H\mathbf{u}_2 \cdots \mathbf{q}_k^H\mathbf{u}_N\right]^T$. Therefore, $\mathbf{r}_i$ for $i \in \{K+1, \ldots, M\}$ has an LP property to that of the rows of $\mathbf{R}_{yy}$, and we can obtain the following expression for $\mathbf{r}_i$ based on (8):

$$\mathbf{r}_k(n) + \sum_{i=1}^{K} c_i \mathbf{r}_k(n-i) = 0, k = 1, \ldots, K, n = K+1, \ldots, N. \tag{10}$$

A Toeplitz matrix $\mathbf{A}$ is defined as follows:

$$\begin{aligned} \mathbf{A} = \mathrm{Toeplitz}\Big(&\left[c_K\ \mathbf{0}_{1\times(N-K-1)}\right]^{\mathrm{T}}, \\ &\left[c_K\ c_{K-1} \cdots c_1\ 1\ \mathbf{0}_{1\times(N-K-1)}\right]\Big), \end{aligned} \tag{11}$$

Then, (10) can be rewritten as:

$$\mathbf{A}\mathbf{r}_k = \mathbf{D}_k\mathbf{c} - \mathbf{f}_k = \mathbf{0}, \quad k = 1, 2, \ldots, K, \tag{12}$$

where

$$\mathbf{D}_k = \begin{bmatrix} [\mathbf{r}_k]_K & [\mathbf{r}_k]_{K-1} & \cdots & [\mathbf{r}_k]_1 \\ [\mathbf{r}_k]_{K+1} & [\mathbf{r}_k]_K & \cdots & [\mathbf{r}_k]_2 \\ \vdots & \vdots & \ddots & \vdots \\ [\mathbf{r}_k]_{N-1} & [\mathbf{r}_k]_{N-2} & \cdots & [\mathbf{r}_k]_{N-K} \end{bmatrix},$$
$$\mathbf{c} = \left[c_1 \; c_2 \; \cdots \; c_K\right]^{\mathrm{T}},$$

and $\mathbf{f}_k = -\left[[\mathbf{r}_k]_{K+1} \; [\mathbf{r}_k]_{K+2} \cdots [\mathbf{r}_k]_N\right]^{\mathrm{T}}$.

Collecting all K vectors in (12) together yields:

$$[(\mathbf{A}\mathbf{r}_1)^{\mathrm{T}} \quad (\mathbf{A}\mathbf{r}_2)^{\mathrm{T}} \quad \cdots \quad (\mathbf{A}\mathbf{r}_K)^{\mathrm{T}}]^{\mathrm{T}} = \mathbf{D}\mathbf{c} - \mathbf{f} = \mathbf{0}, \tag{13}$$

with $\mathbf{D} = [\mathbf{D}_1^{\mathrm{T}} \quad \mathbf{D}_2^{\mathrm{T}} \quad \cdots \quad \mathbf{D}_K^{\mathrm{T}}]^{\mathrm{T}}, \mathbf{f} = [\mathbf{f}_1^{\mathrm{T}} \quad \mathbf{f}_2^{\mathrm{T}} \quad \cdots \quad \mathbf{f}_K^{\mathrm{T}}]^{\mathrm{T}}$. In the absence of noise, it is easy to calculate $\mathbf{c}$ from (13).

Step 1 In the presence of noise, however, $\mathbf{R}_{zz} = \bar{\mathbf{R}}^H \bar{\mathbf{R}} \neq \mathbf{R}_{yy}$. That is, only $\mathbf{R}_{zz}$ is available instead of $\mathbf{R}_{yy}$. Hence, based on the above analysis, QR decomposition is similarly performed on the autocorrelation covariance matrix $\mathbf{R}_{zz}$ to obtain the noisy matrices $\mathbf{Q}$ and $\mathbf{R}$. Therefore, $(\mathbf{D}\mathbf{c} - \mathbf{f})$ in (13) is no longer equal to a zero vector again in the presence of noise. In the following, we define the result of $(\mathbf{D}\mathbf{c} - \mathbf{f})$ as $\mathbf{e} \in \mathbb{C}^{(N-K)K \times 1}$. The resulting problem is converted into the problem of finding $\mathbf{c}$ from $\mathbf{D}\mathbf{c} - \mathbf{f} = \mathbf{e}$, which can be solved by means of the following WLS minimization [1] :

$$\hat{\mathbf{c}} = \arg\min_{\mathbf{c}} \mathbf{e}^H \mathcal{W} \mathbf{e} = \left(\mathbf{D}^H \mathcal{W} \mathbf{D}\right)^{-1} \mathbf{D}^H \mathcal{W} \mathbf{f}, \tag{14}$$

where $\mathcal{W}$ is a symmetric weight matrix, for which the optimal choice is derived from the covariance matrix w.r.t. $\mathbf{e}$, given by

$$\mathcal{W} = \sigma^2 \left[\mathbb{E}\left\{\mathbf{e}\mathbf{e}^H\right\}\right]^{-1} = \mathbf{I}_K \otimes (\mathbf{A}\mathbf{A}^H)^{-1}. \tag{15}$$

Next, by substituting $\hat{\mathbf{c}}$ into (9), an estimate of the steering vector, i.e., $\hat{b}_k$, w.r.t. the elevation angle can be obtained from the roots of (9). Finally, the frequency $\{\hat{\nu}_k\}$ w.r.t. the elevation angle ϕ_k is:

$$\hat{\nu}_k = \angle(\hat{b}_k), k = 1, 2, \ldots, K. \tag{16}$$

Step 2 Similarly, the frequency $\{\mu_k\}$ w.r.t. the azimuth angle θ_k can be computed by using the WLS method based on the QR decomposition of $\mathbf{R}_{zz}^H$. However, this will lead to an unpair match problem for the joint azimuth and elevation angles. To solve this problem, a steering matrix $\mathbf{G}$ based on the estimates of $\hat{b}_k$ is constructed. We have:

$$\mathbf{G} = \left[\mathbf{g}_1 \; \mathbf{g}_2 \cdots \mathbf{g}_K\right], \tag{17}$$

with $\mathbf{g}_k = \left[\hat{b}_k \; \hat{b}_k^2 \; \cdots \; \hat{b}_k^N\right]^{\mathrm{T}}$. Therefore, $\bar{\mathbf{R}}$ is rewritten as:

$$\bar{\mathbf{R}} = \mathbf{H}\boldsymbol{\Gamma}\mathbf{G}^{\mathrm{T}}, \tag{18}$$

where $\boldsymbol{\Gamma} = \mathrm{diag}\left([\gamma_1 \; \gamma_2 \; \cdots \; \gamma_K]\right)$ with $\gamma_k = \mathbb{E}[s_k(t)s_k^H(t)]$, and the matrix $\mathbf{H} = \left[\mathbf{h}_1 \; \mathbf{h}_2 \cdots \mathbf{h}_K\right]$ with $\mathbf{h}_k = \left[a_k \; a_k^2 \; \cdots \; a_k^M\right]^{\mathrm{T}}$. As shown in (18), the steering matrices $\mathbf{G}$ and $\mathbf{H}$, corresponding to the joint azimuth and elevation angles, respectively, are completely separated, with the kth columns of $\mathbf{G}^{\mathrm{T}}$ and $\mathbf{H}$ being characterized only by ν_k and μ_k, respectively. Defining $\hat{\mathbf{P}} = \mathbf{H}\boldsymbol{\Gamma}$, we obtain:

$$\hat{\mathbf{P}} = \bar{\mathbf{R}}(\hat{\mathbf{G}}^{\dagger})^{\mathrm{T}}, \tag{19}$$

where † denotes the pseudoinverse operator. It is worth noting that the elements of $\hat{\mathbf{P}}$, i.e., $\{\mathbf{h}_k\gamma_k\}$, also satisfy the LP property, which leads to the following relationship:

$$\hat{\mathbf{h}}_{k,u}\alpha_k \exp\{j\mu_k\} = \hat{\mathbf{h}}_{k,l}, \tag{20}$$

where $\hat{\mathbf{h}}_{k,u}$ and $\hat{\mathbf{h}}_{k,l}$ are $\hat{\mathbf{p}}_k$ without the last and first elements, respectively, and $\hat{\mathbf{p}}_k = \mathbf{h}_k\gamma_k$. Therefore, the solution to (20) can be calculated using the WLS technique and is given by

$$\hat{a}_k = \frac{\hat{\mathbf{h}}_{k,u}^H \boldsymbol{\Psi}_k \hat{\mathbf{h}}_{k,l}}{\hat{\mathbf{h}}_{k,u}^H \boldsymbol{\Psi}_k \hat{\mathbf{h}}_{k,u}}, \quad k = 1, 2, \ldots, K, \tag{21}$$

where $\boldsymbol{\Psi}_k = \left(\mathbf{B}_k\mathbf{B}_k^H\right)^{-1}$ with the Toeplitz matrix $\mathbf{B}_k$ being given by

$$\mathbf{B}_k = \mathrm{Toeplitz}\left([-a_k \quad \mathbf{0}_{1\times(M-2)}]^{\mathrm{T}}, \quad [-a_k \quad 1 \quad \mathbf{0}_{1\times(M-2)}]\right). \tag{22}$$

As a result, the frequency μ_k is obtained as:

$$\hat{\mu}_k = \angle(\hat{a}_k). \tag{23}$$

Step 3 Now, the joint azimuth and elevation angles θ_k and ϕ_k can be estimated as:

$$\hat{\phi}_k = \cos^{-1}\left(\frac{\lambda}{2\pi d}\hat{\nu}_k\right), \; \hat{\theta}_k = \cos^{-1}\left(\frac{\lambda}{2\pi d}\hat{\mu}_k\right). \tag{24}$$

The joint angles $\hat{\theta}_k$ and $\hat{\phi}_k$ are automatically pair match, and the computational complexity of the proposed method is $O(MN^2 - M^2N + M^3)$.

We summarize the main steps of the proposed algorithm as follows:

(1) QR decomposition is performed on the autocorrelation covariance matrix to obtain the subspace corresponding to ϕ_k (or θ_k).

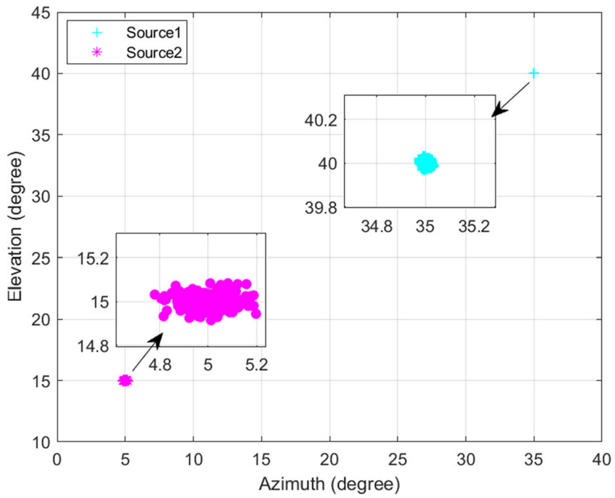

Fig. 2 The scatter plot of estimation $\hat{\theta}$ and $\hat{\phi}$ by the proposed algorithm

(2) The LP property and WLS method are used to obtain an estimate of ϕ_k (or θ_k) from (7) to (16).
(3) The obtained estimate of ϕ_k (or θ_k) is used to construct the steering matrix **G** in (17), and the matrix **P** that contains the information of θ_k (or ϕ_k) is obtained using (19).
(4) The obtained matrix **P** and the WLS method are used to estimate θ_k (or ϕ_k) from (20) to (24).

4 Numerical Examples

Simulation results are presented to evaluate the DOA estimation performance of the proposed algorithm in comparison with the 2-D ESPRIT method [8], the MEMP theomd [6], the PM method [17], Xi's method [18], Liu's method [14], the cross-correlation-based method [16], and the ML method [9] as well as the CRLB [15]. Consider a constant signal power, denoted by σ_s^2. The signal-to-noise ratio (SNR) is defined as SNR $= 10\log(\sigma_s^2/\sigma^2)$. We scale the noise power to produce different SNR conditions. The root mean square error (RMSE), defined as RMSE $= \sqrt{\mathbb{E}\{(\hat{\theta}_k - \theta_k)^2\} + \mathbb{E}\{(\hat{\phi}_k - \phi_k)^2\}}$, is considered as a metric to verify the effectiveness of the proposed method. Our simulations consist of 200 Monte Carlo trials run in the MATLAB R2017b on a laptop with 32 GB of RAM and the 64-bit Windows 10 operating system.

The 2-D DOA distributions at the joint azimuth and elevation angles $(5°, 15°)$ and $(35°, 40°)$ are plotted in Fig. 2, where $M = N = 16$, SNR=10 dB and the number of snapshots is $L = 1000$. As shown in Fig. 2, the proposed algorithm locates the true sources with super-resolution performance. Unless stated otherwise, the parameters settings for the following simulations are the same as in this experiment.

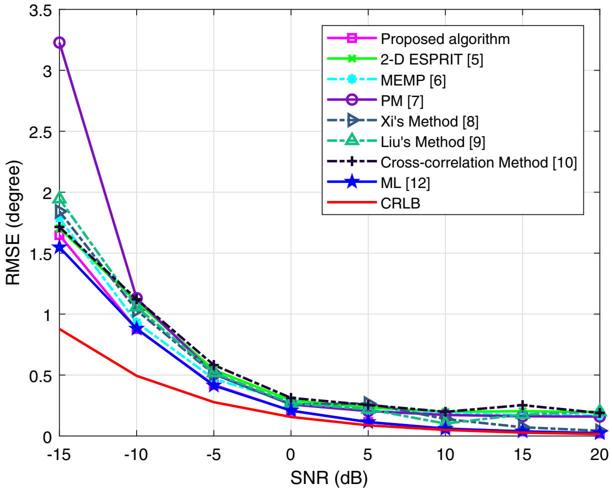

Fig. 3 RMSE of elevation and azimuth versus SNR

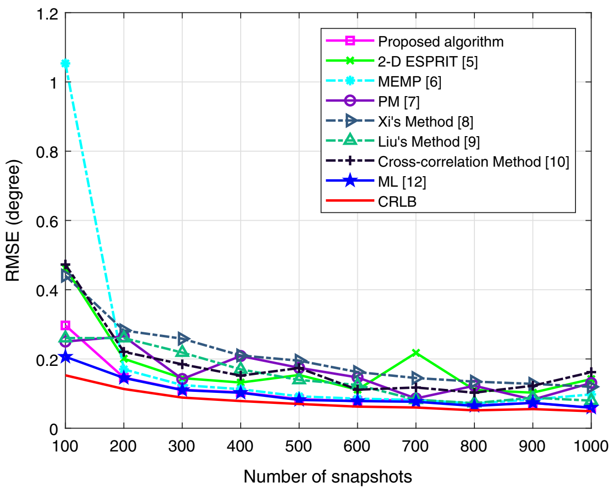

Fig. 4 RMSE of elevation and azimuth versus number of snapshots

In our second test, we investigate the RMSE of the proposed method versus the SNR and the number of snapshots, as shown in Figs. 3 and 4, respectively. Compared with the 2-D ESPRIT method, the MEMP method, the PM method and Xi's method, the proposed method achieves DOA estimation performance comparable to that of the ML method and better than that of other algorithms; in particular, it achieves a higher SNR. Moreover, the proposed solution closely approaches the CRLB when the SNR is larger than 0 dB, as seen in Fig. 3, while it is observed from Fig. 4 that the proposed method outperforms the other compared methods when the number of snapshots is larger than 200 and shows a gradual improvement in DOA estimation performance as the number of snapshots increases.

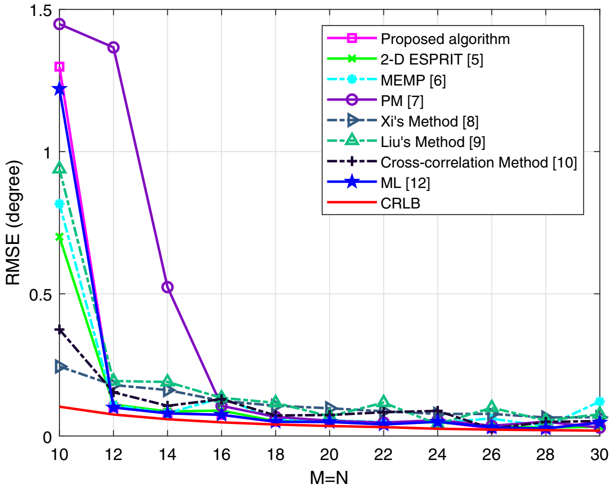

Fig. 5 RMSE of elevation and azimuth versus number of sensors

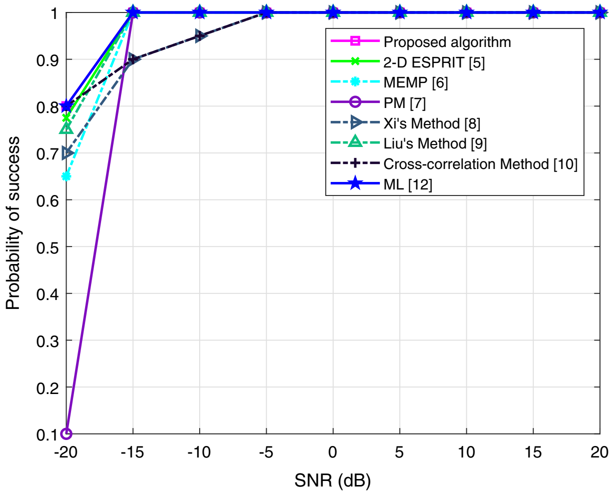

Fig. 6 Probability of success versus SNR

In our third test, the RMSE versus the number of sensors is evaluated, where the number of sensors $M = N$ is varied from 10 to 30, as shown in Fig. 5. The proposed method achieves performance comparable to that of the ML method and is superior to the other algorithms when $M(N) > 12$. With an increasing of number of sensors, all compared methods achieve better DOA estimation performance.

In our fourth test, the probability of success versus the SNR is examined, and the results are plotted in Fig. 6, where the probability of success is computed as the ratio of the number of successful runs to the total number of independent runs. A trial is regarded as a successful one when $\max_{k=1,2} |\hat{\omega}_k - \omega_k| \leq |\omega_2 - \omega_1|/2$, $\omega = \theta$ or ϕ.

Table 1 Computation time (second) versus the number of sensors ($M = N$)

Algorithm	Complexity	$M = 10$	$M = 20$	$M = 30$
Proposed algorithm	$O(M^3)$	0.0010	0.0014	0.0017
2-D ESPRIT [5]	$O(M^2N^2)$	0.0016	0.0127	0.0526
MEMP [6]	$O(M^2N^2)$	0.0024	0.0135	0.0617
PM [7]	$O(MNL)$	0.0016	0.0250	0.1567
Xi's method [8]	$O(MNL + M^2N + N^2M)$	1.5514	1.8962	2.9053
Liu's method [9]	$O(MNL + M^2N)$	0.0025	0.0356	0.1879
Cross-correlation method [10]	$O(MNL)$	0.0016	0.0230	0.1392
ML [12]	$O(M^3N^3)$	0.0431	0.3119	1.0704

It is concluded that all methods achieve 100% success at SNR ≥ -15 dB, and our method and the ML method achieve the highest resolution probability.

The last experiment is to compare the runtimes of the algorithms, as shown in Table 1. The average CPU runtime is used as the performance metric to provide a rough estimate of complexity. For simplicity, we consider only the principal complexity of each method. Both simulation results and the complexity analysis demonstrate that the proposed method is much faster than the other investigated methods. Specifically, the complexity of our method, i.e., $O(M^3)$, is lower than that of the other algorithms for $M = N$.

5 Conclusion

A fast 2-D DOA estimator is designed in which the resulting 2-D DOA estimation problem is converted into a 2-D frequency estimation problem. With the help of the LP property, the frequency w.r.t. the elevation angle is first obtained from the autocorrelation covariance matrix of the received data using the WLS technique. To address the unpair match problem, the frequency w.r.t. the azimuth angle is estimated based on the constructed steering matrix w.r.t. the estimated elevation angle constructed in the first step. Finally, both the azimuth and elevation angles can be easily computed using the corresponding inverse cosine functions. Simulation results show that the proposed method enables more accurate DOA estimation than other methods as well as faster implementation as a result of the ability to obtain closed-form solutions instead of performing iterative approximation.

Acknowledgements This work was jointly supported by Fundamental Research Funds for Central Universities (Grand No. WUT: 2018 IVA 097) and the grant from the National Natural Science Foundation of China (Project No. 61771353).

References

1. F.K.W. Chan, H.C. So, W. Sun, Subspace approach for two-dimensional parameter estimation of multiple damped sinusoids. Signal Process. **92**(9), 2172–2179 (2012)
2. H. Chen, C. Hou, W.-P. Zhu, W. Liu, Y.-Y. Dong, Z. Peng, Q. Wang, ESPRIT-like two-dimensional direction finding for mixed circular and strictly noncircular sources based on joint diagonalization. Signal Process. **141**, 48–56 (2017)
3. A.M. Elbir, Two-dimensional DOA estimation via shifted sparse arrays with higher degrees of freedom. Circuits Syst. Signal Process. **38**, 5549–5575 (2019)
4. A.M. Elbir, V-shaped sparse arrays for 2-D DOA estimation. Circuits Syst. Signal Process. **38**, 2792–2809 (2019)
5. S.F. Hsieh, K.J.R. Liu, K. Yao, Applications of truncated QR methods to sinusoidal frequency estimation, in *Proc. ICASSP.*, vol. 5 (Albuquerque, New Mexico, USA, 1990), pp. 2571–2574
6. Y. Hua, Estimating two-dimensional frequencies by matrix enhancement and matrix pencil. IEEE Trans. Signal Process. **40**(9), 2267–2280 (1992)
7. L. Huang, Y. Wu, H.C. So, Y. Zhang, L. Huang, Multidimensional sinusoidal frequency estimation using subspace and projection separation approaches. IEEE Trans. Signal Process. **60**(10), 5536–5543 (2012)
8. C. Jinli, G. Hong, S. Weimin, Angle estimation using ESPRIT without pairing in MIMO radar. Electron. Lett. **44**, 1422–1423 (2008)
9. T. Li, A. Nehorai, Maximum likelihood direction finding in spatially colored noise fields using sparse sensor arrays. IEEE Trans. Signal Process. **59**(3), 1048–1062 (2011)
10. Q. Liu, Y. Gu, H.C. So, DOA estimation in impulsive noise via low-rank matrix approximation and weakly convex optimization. IEEE Trans. Aerosp. Electron. Syst. **55**(6), 3603–3616 (2019)
11. Q. Liu, W. Wang, D. Liang, X.P. Wang, Real-valued reweighted l_1 norm minimization method based on data reconstruction in MIMO radar. IEICE Trans. Commun. **98**(11), 2307–2313 (2015)
12. Q. Liu, X.P. Wang, Direction of arrival estimation via reweighted l_1 norm penalty algorithm for monostatic MIMO radar. Multidimens. Syst. Signal Process. **29**(2), 733–744 (2018)
13. Q. Liu, H.C. So, G. Yuantao, Off-grid DOA estimation with nonconvex regularization via joint sparse representation. Signal Process. **140**, 170–176 (2017)
14. S. Liu, L. Yang, D. Li, H. Cao, Subspace extension algorithm for 2D DOA estimation with L-shaped sparse array. Multidimens. Syst. Signal. Process. **28**, 315–327 (2017)
15. P. Stoica, K.C. Sharman, Maximum likelihood methods for direction-of-arrival estimation. IEEE Trans. Acoust. Speech Signal Process. **38**(7), 1132–1143 (1990)
16. N. Tayem, K. Majeed, A.A. Hussain, Two-dimensional DOA estimation using cross-correlation matrix with L-shaped array. IEEE Antennas Wirel. Propag. Lett. **15**, 1077–1080 (2015)
17. N. Tayem, H.M. Kwon, L-shape 2-dimensional arrival angle estimation with propagator method. IEEE Trans. Antennas Propag. **53**(5), 1622–1630 (2005)
18. N. Xi, L. Liping, A computationally efficient subspace algorithm for 2-D DOA estimation with L-shaped array. IEEE Signal Process. **21**(8), 971–974 (2014)
19. N. Xi, Q. Guobing, X. Xianbing, Z. Kai, Z. Kesheng, A 2-D DOA estimation algorithm for closely spaced sources with L-shaped array. Circuits Syst. Signal Process. **36**, 4498–4511 (2017)
20. X. Zhang, L. Xu, L. Xu, D. Xu, Direction of departure (DOD) and direction of arrival (DOA) estimation in MIMO radar with reduced-dimension MUSIC. IEEE Commun. Lett. **14**(12), 1161–1163 (2010)
21. G. Zhao, Z. Liu, J. Lin, G. Shi, F. Shen, Wideband DOA estimation based on sparse representation in 2-D frequency domain. IEEE Sens. J. **15**(1), 227–233 (2015)
22. Z. Zheng, S. Mu, Two-dimensional DOA estimation using two parallel nested arrays. IEEE Communications Letters **24**(3), 568–571 (2020)
23. Z. Zheng, W. Wang, Y. Kong, Y.D. Zhang, MISC array: a new sparse array design achieving increased degrees of freedom and reduced mutual coupling effect. IEEE Trans. Signal Process. **67**(7), 1728–1741 (2019)
24. Z. Zheng, W. Wang, H. Meng, H.C. So, H. Zhang, Efficient beamspace-based algorithm for two-dimensional DOA estimation of incoherently distributed sources in massive MIMO systems. IEEE Trans. Veh. Technol. **67**(12), 11776–11789 (2018)